To appear in *Waves in Random and Complex Media*
Vol. 00, No. 00, Month 20XX, 1–23

On effective attenuation in multiscale composite media

Josselin Garnier[a] and Knut Sølna[b]
[a] *Laboratoire de Probabilités et Modèles Aléatoires & Laboratoire Jacques-Louis Lions, Université Paris Diderot, 75251 Paris Cedex 13, France, garnier@math.univ-paris-diderot.fr*
[b] *Department of Mathematics, University of California, Irvine CA 92697, ksolna@math.uci.edu*

(*Received 00 Month 20XX; final version received 00 Month 20XX*)

Experiments show that waves propagating through the earth's crust experience frequency-dependent attenuation. Three regimes have been identified with specific attenuation properties: the low-, mid-, and high-frequency regimes with attenuation in general increasing with frequency. This paper shows how the observed behavior can be explained via theory for waves in random media. It considers multiple scattering of waves propagating in non-lossy one-dimensional random media with short- and/or long-range correlations. Using stochastic homogenization theory it is possible to show that pulse propagation is described by effective fractional damping exponents. The damping exponents are related to the Hurst parameters of the random media which are characteristic parameters of the correlation properties of the fluctuations of the random media. This description is the link in between the random medium properties and the observed damping behavior. In particular a simple binary medium is shown to reproduce well the experimental attenuation properties in the low-, mid-, and high-frequency regimes.

Keywords: acoustic waves, attenuation and dispersion, random media, self-similar processes

1. Introduction

When a wave propagates through the earth's crust it is scrambled by scattering associated with the microstructure. In fact scrambling may appear as an attenuation of the wave front as it modulates and spreads out its profile and transfers its coherent energy to incoherent coda waves which are of small amplitude relative to the wave front. This transformation depends on the "roughness" of the medium fluctuations and it has been characterized as "apparent attenuation". In complicated sections of the earth's crust we cannot hope to identify perfectly the medium parameters at each point, however, by looking at well data outcrops for instance we may be able to describe the statistics of the microstructure. This is the point of view taken in this paper, we model the medium as being random and then we ask the question how can we describe the apparent attenuation. That is we model the medium fluctuations, the microstructure, as being random, in fact, a realization of a stochastic process. A main point is that by doing so we describe wave propagation in a *wide class of media*, because, as it turns out only the covariance of the medium fluctuations is important in order to characterize the apparent attenuation phenomenon. We will here consider wave propagation in the context of a specific

medium model, a piecewise constant medium, but hasten to add that the results are general in the sense of characterizing the apparent attenuation phenomenon in all media whose covariance has similar properties as the ones we discuss below for our example medium.

Experimental observations show that the attenuation coefficient Q^{-1} defined through the transmission coefficient by

$$|T(\omega, z)|^2 = \exp\Big(- \frac{|\omega|}{c_0} Q^{-1}(\omega) z \Big)$$

has a frequency dependence of the form

$$Q^{-1}(\omega) \approx |\omega|^{\alpha}, \tag{1}$$

where $\alpha \in (-1, 1)$ is a parameter that is characteristic of the medium and obtained through a fitting of measured data. In particular, it is reported for body waves an exponent $\alpha \simeq 0.4$ for very low frequencies $< 10^{-3}$Hz [27], $\alpha \in (-0.4, 0)$ in the range $(10^{-3}, 1)$Hz [10, 36], and $\alpha \simeq -1$ for higher frequencies $>$ 1Hz [10, 12]. We will return to this picture in Section 3.7. In this paper we show how such a picture can be explained in terms of scattering by a multiscale medium with short- and long-range correlation properties and show that such a medium can produce these types of behaviors. In particular we propose a simple binary random medium model (i.e. a medium made of two materials) that can reproduce simultaneously the three frequency-dependent power laws observed experimentally in the low-, mid- and high-frequency bands. Our focus in this paper is on how the observed attenuation can be explained in terms of a scattering picture. However, in many situations there may also be anelastic attenuation present and we comment on such attenuation in Section 3.8. The question as to which of the two attenuation mechanisms is dominant is still partly open in many wave propagation scenarios. The analysis presented in this paper contributes to the understanding of this issue by presenting in detail a characterization of the damping in the case of scattering only.

2. Acoustic Wave Propagation in One-Dimensional Random Media

2.1. *Acoustic Wave Equations*

We present here a stochastic model for the acoustic wave equations in the presence of random fluctuations of the medium with short- or long-range correlations. The one-dimensional acoustic wave equations are given by

$$\rho(z) \frac{\partial u}{\partial t} + \frac{\partial p}{\partial z} = 0\,, \tag{2}$$

$$\frac{1}{K(z)} \frac{\partial p}{\partial t} + \frac{\partial u}{\partial z} = 0\,, \tag{3}$$

where t is the time variable, z the one-dimensional space variable, p is the pressure field, and u is the velocity field. For simplicity we assume that the density of the medium ρ is a constant equal to ρ_0. The bulk modulus of the medium K is assumed to be randomly varying in the region $z \in [0, L]$ and we consider the weakly heterogeneous regime [16], in which the fluctuations of the bulk modulus are small

and rapid (compared to the propagation distance):

$$\frac{1}{K(z)} = \begin{cases} \frac{1}{K_0}\big(1+\nu(z)\big), & z \in [0,L]\,, \\ \frac{1}{K_0}, & z \in (-\infty,0)\cup(L,\infty)\,, \end{cases} \tag{4}$$

$$\rho(z) = \rho_0 \quad \text{for all} \quad z\,. \tag{5}$$

We consider here the case with constant density. The case with also varying density is discussed in [16] and give results that are similar to the case with varying bulk modulus from the point of view of attenuation. The effective impedance and speed of sound are $\zeta_0 = \sqrt{K_0\rho_0}$ and $c_0 = \sqrt{K_0/\rho_0}$, respectively. The random process ν is assumed to be stationary and to have mean zero. Its covariance, or auto-correlation, function is denoted by

$$\phi(z) = \mathbb{E}[\nu(z')\nu(z'+z)]\,, \tag{6}$$

where $\mathbb{E}$ stands for the expectation with respect to the distribution of the random medium. The function $\phi(z)$ is bounded, even, and maximal at zero ($\phi(0)$ is the variance of the fluctuations). Its local regularity or smoothness at zero and its asymptotic behavior at infinity characterize the short- and long-range correlations of the random medium, as we discuss in the next subsection. As we will see below the properties of the covariance function are the ones that give the "apparent" attenuation properties of the scattering due to the microstructure.

2.2. *Random Medium Properties*

Wave propagation in random media is usually studied when the process ν modeling the medium fluctuations has *mixing* properties [16]. Mixing means that the random values $\nu(z'+z)$ and $\nu(z')$ taken at two points separated by the distance z become rapidly uncorrelated when $z \to \infty$. More precisely we say that the random process ν is mixing if its covariance function $\phi(z)$ decays fast enough at infinity so that it is integrable:

$$\int_0^\infty |\phi(z)|dz < \infty\,. \tag{7}$$

The mixing property of the medium may be thought of as characterizing the large scale features of the medium. The local behavior or regularity is also important. Regarding the local or small-scale behavior it is usually assumed that the covariance function is Lipschitz continuous, ie, there is a constant K so that for all z

$$|\phi(z+\Delta z) - \phi(z)| \le K|\Delta z|\,.$$

In the case of a piecewise constant medium Lipschitz continuity of the process corresponds to that there is at most one jump within a small interval (no accumulation of jumps). In the context of the random process ν we say here that it is *regular* (Lipschitz continuous) if its covariance function satisfies:

$$\phi(z) \overset{|z|\ll\ell_c}{\simeq} \phi(0)\Big(1 - d_{1/2}\Big|\frac{z}{\ell_c}\Big| + o\Big(\Big|\frac{z}{\ell_c}\Big|\Big)\Big)\,, \tag{8}$$

where $d_{1/2} > 0$ and $\ell_c > 0$ is a length.

We remark that if in fact the process ν is stationary and differentiable, so that we have a *smooth* random medium, then

$$\phi(z) \overset{|z|\ll\ell_c}{\simeq} \phi(0)\Big(1+O\Big(\Big|\frac{z}{\ell_c}\Big|^2\Big)\Big)\,. \tag{9}$$

However, here we shall consider media with jumps and thus non-smooth random media.

These are the usual assumptions for random media, under which the theory is well established. The O'Doherty-Anstey theory then describes the propagating pulse in these regimes. The effective equation for the wave front has been obtained by several authors [7, 8, 11, 16, 28, 30, 38]. The pulse propagation is characterized by a random time shift and a deterministic spreading. The random time shift is described in terms of a standard Brownian motion, while the deterministic spreading is described by a pseudo-differential operator.

Wave propagation in multiscale and rough media, with short- or long-range fluctuations, has recently attracted a lot of attention, as more and more data collected in real environments confirm that this situation can be encountered in many different contexts, such as in geophysics [13, 35] or in laser beam propagation through the atmosphere [14, 17, 37].

Qualitatively, the long-range correlation property means that the random process has long memory (in contrast with a mixing process). This means that the correlation degree between the random values $\nu(z'+z)$ and $\nu(z')$ taken at two points separated by the distance z decays only slowly when $z\to\infty$, or equivalently that the covariance function has a slow decay at infinity. More precisely we say that the random process ν has the H'-long-range correlation property if its covariance function satisfies:

$$\phi(z) \overset{|z|\gg\ell_c}{\simeq} \phi(0) r_{H'} \Big|\frac{z}{\ell_c}\Big|^{2H'-2}, \tag{10}$$

where $r_{H'}>0$ and $H'\in(1/2,1)$. The parameter H' is sometimes referred to as the Hurst exponent. Here ℓ_c is the critical length scale beyond which the power law behavior (10) is valid. Note that the covariance function is not integrable since $2H'-2\in(-1,0)$, which means that a random process with the H'-long-range correlation property is not mixing.

Qualitatively the short-range correlation property means that the random process is rough at small scales. This means that the correlation degree between the random values $\nu(z'+z)$ and $\nu(z')$ taken at two points separated by the distance z has a sharp decay at zero. It corresponds to the fact that the covariance function decays faster than an affine function at zero. More precisely we say that the random process ν has the H-short-range correlation property if its covariance function satisfies:

$$\phi(z) \overset{|z|\ll\ell_c}{\simeq} \phi(0)\Big(1-d_H\Big|\frac{z}{\ell_c}\Big|^{2H}+O\Big(\frac{|z|}{\ell_c}\Big)\Big)\,, \tag{11}$$

where $d_H>0$ and $H\in(0,1/2)$. Here ℓ_c is the critical length scale below which the power law behavior (11) is valid. Additional technical hypotheses on the differentiability of ϕ are necessary for the mathematical proof (see Appendix B [19]). We simply mention here that these technical hypotheses are satisfied by the models presented in the next subsection.

2.3. *Binary Random Medium Models with Short- and/or Long-range Correlation Properties*

In this section we present the random processes ν that model the random medium fluctuations as function of position $z \in (0, L)$. Indeed we are interested in characterizing the apparent attenuation and the central quantity that characterizes this phenomenon is the covariance of this random process, therefore we here discuss this medium covariance in detail. The random process modeling the medium fluctuations that we will be considering corresponds to a binary medium which means that the process ν is stepwise constant and takes values $\pm\sigma$ over intervals with random lengths. In fact how these lengths are modeled statistically is what is important and is what will differentiate the three regimes. We again remind the reader that we use a specific model for the medium fluctuations to illustrate but that the results that we will present below are general and valid in fact for all media that the share the same correlation properties as the ones we are about to present.

Binary medium with mixing and regular properties. Here we construct a process corresponding to a binary medium so that the process ν takes values $\pm\sigma$ over intervals with random lengths. We denote by $(l_j)_{j\geq 0}$ the lengths of these intervals and by $(n_j)_{j\geq 0}$ the values taken by the process over each elementary interval. The process $\nu(z)$ is defined by

$$\nu(z) = n_{N_z} \text{ where } N_z = \sup\{n \geq 0,\, L_n \leq z\}\,, \tag{12}$$

with $L_0 = 0$ and $L_{n+1} = L_n + l_n$. The random variables n_j are independent and identically distributed (i.i.d.) with the distribution

$$\mathbb{P}(n_1 = \pm\sigma) = \frac{1}{2}\,. \tag{13}$$

The random variables l_j are i.i.d. with the exponential distribution whose probability density function (pdf) is

$$p_{l_1}(z) = \frac{1}{\ell_c}\exp\Big(-\frac{z}{\ell_c}\Big)\mathbf{1}_{[0,\infty)}(z)\,. \tag{14}$$

Note that it is very easy to simulate the random variable l_1, since $-\ell_c \ln U$ has the pdf (14) if U is uniformly distributed over $[0, 1]$. The random process $\nu(z)$ is a stationary jump Markov process and its covariance function is

$$\phi(z) = \sigma^2 \exp\Big(-\frac{|z|}{\ell_c}\Big)\,, \tag{15}$$

which shows that it is a mixing process. The exponential decay means indeed that this covariance function is integrable. This is also the case for the so-called von-Kármán correlation function with decays as $\phi(z) \propto z^{\mu}\exp(-z/\ell_c)$ for relatively large values of the argument and which is sometimes used to model the scaling behavior of complex geology [25]. This will be qualitatively different for the long-range processes we discuss below that has only power law decay at infinity. Note also that the covariance function (15) satisfies

$$\phi(z) \overset{|z|\ll\ell_c}{\simeq} \sigma^2\Big(1 - \frac{|z|}{\ell_c} + o\Big(\frac{|z|}{\ell_c}\Big)\Big)\,, \tag{16}$$

which means this is a regular process.

Our interest is now how the medium fluctuations affect and transform the wave as it propagates. As we discuss in Section 3 this transformation can be described in terms of the covariance function $\phi(z)$. Thus, different media with the same covariance function would lead to similar transformations of the wave. In particular the random variables n_j describing the medium fluctuation in section j could be a general zero mean random variable, not necessarily a discrete random variable, and in this case σ^2 in (16) would be the variance of this random variable. We remark that we actually could have used (continuous) fractional processes, like fractional Ornstein-Uhlenbeck processes, to create short- and long-range correlations.

Binary medium with long-range correlation property. The long-range correlation property for a binary medium corresponds to the existence of intervals much longer than the average interval length. We again consider the process defined by Eq. (12) corresponding to a binary medium where the random variables n_j are i.i.d. with the distribution (13) and the random variables l_j are i.i.d. with the distribution with the Pareto pdf

$$p_{l_1}(z) = (3-2H')\frac{\ell_{\rm c}^{3-2H'}}{z^{4-2H'}}\mathbf{1}_{[\ell_{\rm c},\infty)}(z)\,, \tag{17}$$

where $H' \in (1/2, 1)$. Note that the decay of the pdf is of power law form rather than exponential as in (14), this is sometimes referred to as a "heavy-tailed" distribution. Note that it is very easy to simulate the random variable l_1, since $\ell_{\rm c}U^{-1/(3-2H')}$ has the pdf (17) if U is uniformly distributed over $[0, 1]$. The average length of the random interval is

$$\mathbb{E}[l_1] = \frac{3-2H'}{2-2H'}\ell_{\rm c}\,, \tag{18}$$

while the variance of l_1 is infinite. A salient aspect of this model is that very long intervals (i.e. much longer than $\mathbb{E}[l_1]$) can be generated, which are responsible for the infinite variance of the length of the interval and for the long-range correlation property of the random medium. Moreover, as H' increases from $1/2$ to 1 we see that the long range character becomes relatively stronger with the pdf decaying slower. The process ν is bounded, it has mean zero and variance σ^2. Using renewal theory [15, Eq. (4.6)], the distribution of the process $(\nu(x+z))_{z\geq 0}$ converges to a stationary distribution when $x \to \infty$ and the covariance function of ν satisfies

$$\mathbb{E}[\nu(x)\nu(x+z)] \overset{x\to\infty}{\longrightarrow} \phi(z) = \sigma^2 \int_z^\infty \frac{\mathbb{P}(l_1 > s)}{\mathbb{E}[l_1]} ds\,.$$

The covariance function

$$\phi(z) = \sigma^2\Big[\frac{1}{3-2H'}\frac{\ell_{\rm c}^{2-2H'}}{|z|^{2-2H'}}\mathbf{1}_{[\ell_{\rm c},\infty)}(|z|) + \Big(1 - \frac{2-2H'}{3-2H'}\frac{|z|}{\ell_{\rm c}}\Big)\mathbf{1}_{[0,\ell_{\rm c})}(|z|)\Big]\,, \tag{19}$$

satisfies the H'-long-range correlation property (10) for $|z| \in [\ell_{\rm c}, \infty)$ with $r_{H'} = 1/(3-2H')$. We show a realization of ν in Figure 1 in the top plot for $H' = .75$ and the corresponding covariance function in the bottom plot.

Binary medium with short-range correlation property. The short-range correlation property for a binary medium corresponds to the accumulation of in-

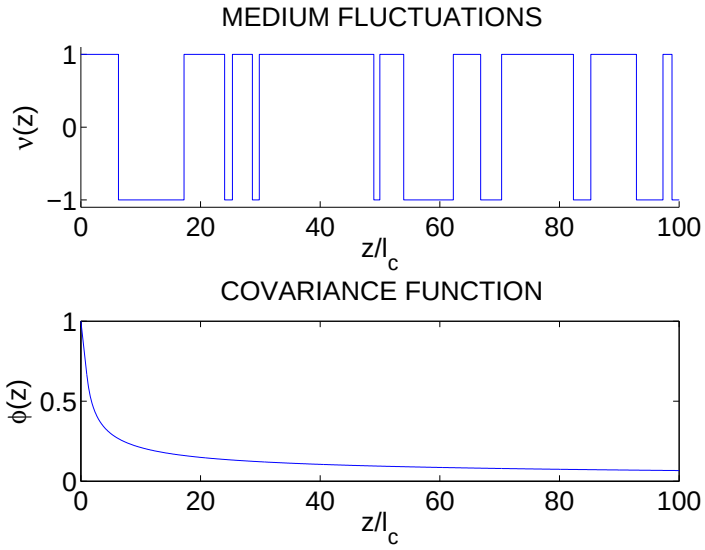

Figure 1. Realization of a binary medium with long-range correlation property, top plot. The covariance function is shown in the bottom plot.

tervals with lengths much smaller than the average length. We again consider the process defined by Eq. (12) corresponding to a binary medium where the random variables n_j are i.i.d. with the distribution (13) and the random variables l_j are i.i.d. with the distribution whose pdf is

$$p_{l_1}(z) = \frac{1-2H}{(\ell_{\rm i}/\ell_{\rm c})^{2H-1}-1}\frac{\ell_{\rm c}^{1-2H}}{z^{2-2H}}\mathbf{1}_{[\ell_{\rm i},\ell_{\rm c}]}(z)\,, \tag{20}$$

where $H \in (0,1/2)$ and $0 < \ell_{\rm i} < \ell_{\rm c}$. Here the inner scale $\ell_{\rm i}$ is introduced in order to obtain a well-defined and normalized pdf and it will be taken to be much smaller than $\ell_{\rm c}$ later on. We introduce the ratio

$$\delta = \frac{\ell_{\rm i}}{\ell_{\rm c}}, \tag{21}$$

that belongs to $(0,1)$. Note that it is very easy to simulate the random variable l_1, since $\ell_{\rm i}[1-(1-\delta^{1-2H})U]^{-1/(1-2H)}$ has the pdf (20) if U is uniformly distributed over $[0,1]$. The average length of the random interval is

$$\mathbb{E}[l_1] = \frac{1-2H}{2H}\frac{1-\delta^{2H}}{\delta^{2H-1}-1}\ell_{\rm c}\,, \tag{22}$$

and its variance is finite. A salient aspect of this model is that it exhibits an accumulation of very small intervals (i.e. much smaller than $\mathbb{E}[l_1]$) which corresponds to very rapid changes in the medium properties. Using renewal theory the distribution of the process $(\nu(x+z))_{z\geq 0}$ converges to a stationary distribution when $x \to \infty$ and the covariance function of ν satisfies

$$\mathbb{E}[\nu(x)\nu(x+z)] \stackrel{x\to\infty}{\longrightarrow} \phi(z)\,, \tag{23}$$

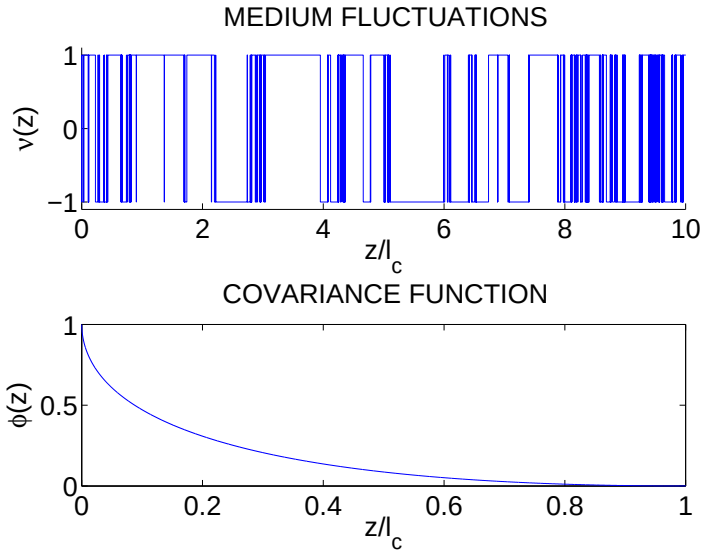

Figure 2. Realization of a binary medium with short-range correlation property, top plot. The covariance function is shown in the bottom plot.

where

$$\phi(z) = \frac{\sigma^2}{1-\delta^{2H}}\Big(1 - \frac{1}{1-2H}\frac{|z|^{2H}}{\ell_{\rm c}^{2H}} + \frac{2H}{1-2H}\frac{|z|}{\ell_{\rm c}}\Big)\mathbf{1}_{(\ell_{\rm i},\ell_{\rm c}]}(|z|)$$
$$+\sigma^2\Big(1 - \frac{2H}{1-2H}\frac{\delta^{2H}-\delta}{1-\delta^{2H}}\frac{|z|}{\ell_{\rm i}}\Big)\mathbf{1}_{[0,\ell_{\rm i}]}(|z|)\,. \tag{24}$$

If $\delta \ll 1$ (i.e. $\ell_{\rm i} \ll \ell_{\rm c}$), then, for $\ell_{\rm i} \le |z| \le \ell_{\rm c}$, we have

$$\phi(z) \simeq \sigma^2\Big(1 - \frac{1}{1-2H}\frac{|z|^{2H}}{\ell_{\rm c}^{2H}} + \frac{2H}{1-2H}\frac{|z|}{\ell_{\rm c}}\Big)\,, \tag{25}$$

which satisfies the H-short-range correlation property (11) for $|z| \in [\ell_{\rm i}, \ell_{\rm c}]$ with $d_H = 1/(1-2H)$.
We show a realization of ν in Figure 2 in the top plot for $H = .25$ and the corresponding covariance function in the bottom plot.

Binary medium with short- and long-range correlation properties. We again consider the process defined by Eq. (12) corresponding to a binary medium where the random variables n_j are i.i.d. with the distribution (13) and the random variables l_j are i.i.d. with the distribution with the pdf

$$p_{l_1}(z) = \Big(1 - a\delta^{1-2H}\Big)\frac{1-2H}{\delta^{2H-1}-1}\frac{\ell_{\rm c}^{1-2H}}{z^{2-2H}}\mathbf{1}_{[\ell_{\rm i},\ell_{\rm c}]}(z)$$
$$+a\delta^{1-2H}(3-2H')\frac{\ell_{\rm c}^{3-2H'}}{z^{4-2H'}}\mathbf{1}_{[\ell_{\rm c},\infty)}(z)\,, \tag{26}$$

where $H \in (0, 1/2)$, $H' \in (1/2, 1)$, $a \in (0, 1)$, and $0 < \ell_{\rm i} < \ell_{\rm c}$. The statistical distribution of the length of the elementary interval is a mixture of the two distributions introduced above in Equations (17) and (20), which means the pdf is supported in $(\ell_{\rm i}, \infty)$, it has a power law decay of the form z^{2H-2} for $z \in [\ell_{\rm i}, \ell_{\rm c}]$ (with $2H-2 \in (-2,-1)$) and of the form $z^{2H'-4}$ for $z \in [\ell_{\rm c}, \infty)$ (with $2H'-4 \in (-3,-2)$).

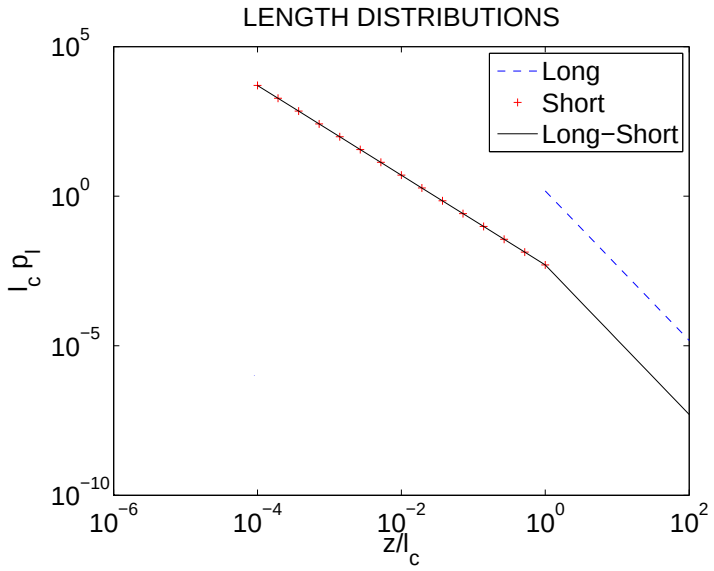

Figure 3. The pdf of the length of the elementary interval for a binary medium with short- and long-range properties, with both accumulation of small intervals and existence of large intervals. Here $H = 0.25$, $H' = 0.75$, $\ell_{\rm i}/\ell_{\rm c} = 0.0001$ and a is chosen as in (27). The figure shows $\ell_{\rm c} p_{l_1}$ by the solid black line (as function of $z/\ell_{\rm c}$), the corresponding short interval length pdf by the red crosses and the long interval pdf by the dashed blue line.

The pdf is continuous at $\ell_{\rm c}$ if we choose a as

$$\frac{1}{a} = \frac{3-2H'}{1-2H} - 2\delta^{1-2H}\frac{1+H-H'}{1-2H}\,, \tag{27}$$

however this is not required in our analysis, we may choose any number in $(0,1)$. The pdf is plotted in Figure 3.

As a result we have both accumulation of very small intervals (much smaller than the mean $\mathbb{E}[l_1]$) and generation of very long intervals (much larger than the mean $\mathbb{E}[l_1]$). Here the mean is

$$\begin{aligned}\mathbb{E}[l_1] &= \Big(1-a\delta^{1-2H}\Big)\frac{1-2H}{2H}\frac{1-\delta^{2H}}{\delta^{2H-1}-1}\ell_{\rm c} + a\delta^{1-2H}\frac{3-2H'}{2-2H'}\ell_{\rm c} \\ &\overset{\ell_{\rm c}\gg\ell_{\rm i}}{\simeq} \Big(\frac{1-2H}{2H} + a\frac{3-2H'}{2-2H'}\Big)\delta^{1-2H}\ell_{\rm c}\,.\end{aligned} \tag{28}$$

The (continuous) covariance function has both H-short-range and H'-long-range properties:
- if $|z| \geq \ell_{\rm c}$, then

$$\begin{aligned}\phi(z) &= \frac{\sigma^2\ell_{\rm c}a}{\mathbb{E}[l_1](2-2H')}\delta^{1-2H}\frac{\ell_{\rm c}^{2-2H'}}{|z|^{2-2H'}} \\ &\overset{\ell_{\rm c}\gg\ell_{\rm i}}{\simeq} \frac{a\sigma^2}{(2-2H')\big(\frac{1-2H}{2H}+a\frac{3-2H'}{2-2H'}\big)}\frac{\ell_{\rm c}^{2-2H'}}{|z|^{2-2H'}}\,,\end{aligned} \tag{29}$$

which shows it has the H'-long-range property in the range $|z| \in [\ell_c, \infty)$ with

$$r_{H'} = \frac{a}{(2-2H')\left(\frac{1-2H}{2H} + a\frac{3-2H'}{2-2H'}\right)}\,.$$

- if $\ell_i \le |z| \le \ell_c$, then

$$\begin{aligned}\phi(z) &= \frac{\sigma^2\ell_c}{\mathbb{E}[l_1]}\delta^{1-2H}\Big\{a\Big(\frac{3-2H'}{2-2H'} - \frac{|z|}{\ell_c}\Big) \\ &\quad + \frac{1-a\delta^{1-2H}}{1-\delta^{1-2H}}\Big[\frac{1}{2H}\Big(1-\frac{|z|^{2H}}{\ell_c^{2H}}\Big) - \Big(1-\frac{|z|}{\ell_c}\Big)\Big]\Big\} \qquad (30)\\ &\overset{\ell_c \gg \ell_i}{\simeq} \frac{\sigma^2}{\left(\frac{1-2H}{2H} + a\frac{3-2H'}{2-2H'}\right)}\Big\{\Big(a\frac{3-2H'}{2-2H'} + \frac{1-2H}{2H}\Big) + (1-a)\frac{|z|}{\ell_c} - \frac{1}{2H}\frac{|z|^{2H}}{\ell_c^{2H}}\Big\}\,,\end{aligned}$$

which shows it has the H-short-range property in the range $|z| \in [\ell_i, \ell_c]$ with

$$d_H = \frac{1}{2H\left(\frac{1-2H}{2H} + a\frac{3-2H'}{2-2H'}\right)}\,.$$

- if $|z| < \ell_i$, then

$$\begin{aligned}\phi(z) &= \frac{\sigma^2\ell_c}{\mathbb{E}[l_1]}\Big\{\delta\Big(1-\frac{|z|}{\ell_i}\Big) + a\delta^{1-2H}\Big(\frac{3-2H'}{2-2H'} - \delta\Big) \\ &\quad + \delta^{1-2H}\frac{1-a\delta^{1-2H}}{1-\delta^{1-2H}}\Big[\frac{1}{2H}\Big(1-\delta^{2H}\Big) - (1-\delta)\Big]\Big\} \qquad (31)\\ &\overset{\ell_c \gg \ell_i}{\simeq} \sigma^2\Big\{1 - \frac{1}{\left(\frac{1-2H}{2H} + a\frac{3-2H'}{2-2H'}\right)\delta^{1-2H}}\frac{|z|}{\ell_c}\Big\}\,,\end{aligned}$$

which shows it has the regular property in the range $|z| \in [0, \ell_i]$. We show a realization of ν in Figure 4 in the top plot for $H = .25, H' = .75$ and the corresponding covariance function in the bottom plot. Note the coexistence of long and accumulation of short intervals.

3. Analysis of the Effective Transmission Coefficient

For the type of random medium fluctuations introduced in the previous section we want to discuss how this gives rise to an apparent attenuation. We discuss this in terms of the binary medium we have introduced, but hasten to add that it is the behavior of the medium covariance function, its decay at infinity and its singular behavior at the origin that are important, in respectively the low- and high-frequency regimes (more precisely we consider high- and low-wavenumber regimes relative to $1/\ell_c$). Thus, the results that we present next carries over to general media with a covariance function having the properties introduced in Section 2.2.

3.1. *Apparent Attenuation in Wave Propagation*

Let us discuss briefly the notion of apparent attenuation and its parameterization. The time-harmonic wave equation or Helmholtz equation deriving from the acoustic

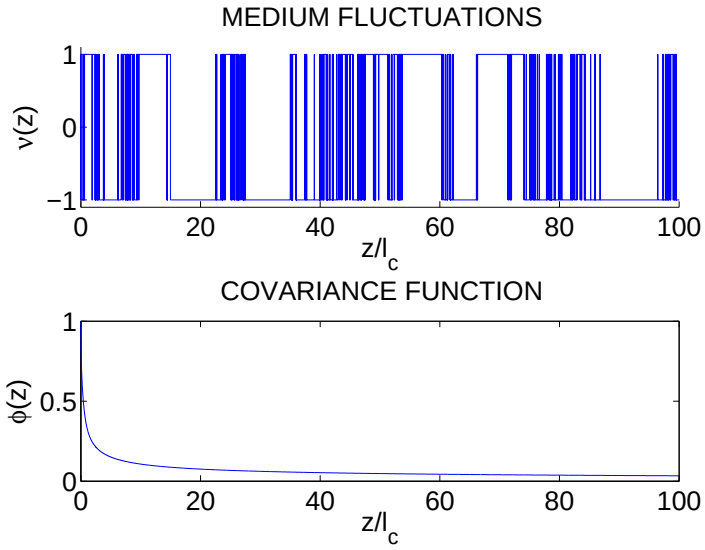

Figure 4. Realization of a binary medium with long- and short-range correlation property, top plot. The covariance function is shown in the bottom plot.

equations Eq. (4) is

$$\frac{\partial^2 \hat{u}}{\partial z^2} + \left(\frac{\omega}{c_0}\right)^2 (1 + \nu(z))\hat{u} = 0\,,$$

We now state some fundamental results that characterize the effective wave propagation through a random medium. In a certain parameter regime we can associate the wave propagation with an effective (time-harmonic) transmission coefficient that indeed depends on only the covariance function of the medium fluctuations ν. Note that this transmission coefficient is in fact a random quantity. The precise sense in which we have convergence to an effective transmission coefficient is addressed in [16] and here simply state that the transmission coefficient is, up to a random phase of the form $i\omega\tau(z)$ corresponding to a random time shift, of the form

$$T(\omega, z) = \exp\Big(- \frac{\gamma_c(\omega)\omega^2}{8c_0^2} z - i\frac{\gamma_s(\omega)\omega^2}{8c_0^2} z\Big)\,. \tag{32}$$

where

$$\gamma_c(\omega) = 2\int_0^\infty \phi(z)\cos\Big(\frac{2\omega z}{c_0}\Big)dz\,, \tag{33}$$

$$\gamma_s(\omega) = 2\int_0^\infty \phi(z)\sin\Big(\frac{2\omega z}{c_0}\Big)dz\,. \tag{34}$$

The term $\exp[-i\gamma_s(\omega)\omega^2 z/(8c_0^2)]$ is a frequency-dependent phase modulation and $\gamma_s(\omega)$ is conjugate to $\gamma_c(\omega)$. This shows that the transmitted wave front when centered with respect to the random travel time correction propagates in a dispersive effective medium with the frequency-dependent wavenumber given by

$$k(\omega) = \frac{\omega}{c_0} - \frac{\gamma_s(\omega)\omega^2}{8c_0^2}\,. \tag{35}$$

Moreover, there is a frequency-dependent attenuation

$$\frac{|\omega|}{c_0}Q^{-1}(\omega) = \frac{\gamma_c(\omega)\omega^2}{4c_0^2}\,, \tag{36}$$

that is always nonnegative by Bochner's theorem because $\gamma_c(\omega)$ is the power spectral density of the fluctuations $\nu(z)$ of the random medium. We also introduce the dispersion function

$$\frac{\omega}{c_0}\mathcal{D}(\omega) = \frac{\gamma_s(\omega)\omega^2}{4c_0^2} \tag{37}$$

that is the conjugate of the attenuation factor.

Regarding the parametrization in terms of the "quality factor" Q we remark that if we consider the damped wave equation, the analogue of the damped harmonic oscillator with damping ratio Q^{-1}:

$$\frac{\partial^2\hat{u}}{\partial z^2} + \left(\frac{\omega}{c_0}\right)Q^{-1}\frac{\partial\hat{u}}{\partial z} + \left(\frac{\omega}{c_0}\right)^2\hat{u} = 0\,,$$

then in the underdamped case we have

$$|T(\omega,z)|^2 = \exp\Big(-\frac{\omega}{c_0}Q^{-1}z\Big)\,. \tag{38}$$

We introduce next a reference and a *normalized frequency* v by:

$$\omega_c = \frac{c_0}{\ell_{\rm c}}, \quad v = \frac{|\omega|}{\omega_c}\,,$$

and find that in normalized coordinates the *attenuation factor* $Q_{\rm e}^{-1}$ and *dispersion function* $\mathcal{D}_{\rm e}$ can be written:

$$Q_{\rm e}^{-1}(v) = Q^{-1}(v\omega_c) = \frac{v}{2}\int_0^\infty \phi(\ell_{\rm c}u)\cos(2vu)du\,, \tag{39}$$

$$\mathcal{D}_{\rm e}(v) = \mathcal{D}(v\omega_c) = \frac{v}{2}\int_0^\infty \phi(\ell_{\rm c}u)\sin(2vu)du\,. \tag{40}$$

Below we discuss how the attenuation factor is affected by the correlation properties of the medium fluctuations. We review first the classic cases of mixing and regular media before we turn our attention to our main cases of interest: media with long- and short-range correlation properties.

3.2. *Random Media with Mixing Properties*

In this subsection we consider the case of a mixing random medium. We assume that the wavenumber ω/c_0 is such that $v \ll 1$. This condition means that the typical wavelength is longer than $\ell_{\rm c}$ and in this case we find that

$$Q_{\rm e}^{-1}(v) = \frac{v}{2}\int_0^\infty \phi(\ell_{\rm c}u)du\,, \qquad \mathcal{D}_{\rm e}(v) = 0\,, \qquad v \ll 1\,, \tag{41}$$

which shows that we have an effective attenuation of the form of Eq. (1) with $\alpha = 1$ and no effective dispersion. Note that here we considered the low-frequency regime so that only the integrated medium covariance function is important. In the regime of relatively high frequencies the behavior of the covariance function at the origin becomes important and we consider this case next.

3.3. *Random Media with Regular Properties*

We consider the case of a random medium with the affine decay behavior at zero:

$$\phi(z) \stackrel{|z|\ll\ell_c}{=} \phi(0)\Big(1 - d_{1/2}\frac{|z|}{\ell_c} + o\Big(\frac{|z|}{\ell_c}\Big)\Big)\,, \tag{42}$$

with $d_{1/2} > 0$. The affine decay (42) of the covariance function is typical of a Markov process, such as the binary medium process in the case in which the lengths of the intervals have an exponential distribution. This behavior is in fact fairly general. For instance the affine decay (42) holds for the binary medium process in the case in which the lengths of the intervals have positive finite expectation. If we assume that the wavenumber ω/c_0 is such that $v \gg 1$, which means that the typical wavelength is smaller than ℓ_c, then we have (see Appendix A [19])

$$\frac{\gamma_c(\omega)\omega^2}{c_0^2} = \frac{\phi(0)d_{1/2}}{2\ell_c}\,, \qquad \frac{\gamma_s(\omega)\omega^2}{c_0^2} = \frac{\phi(0)\omega}{c_0}\,, \tag{43}$$

so that

$$Q_e^{-1}(v) = \frac{1}{v}\frac{\phi(0)d_{1/2}}{8}\,, \qquad \mathcal{D}_e(v) = \frac{\phi(0)}{4}\,, \qquad v \gg 1\,,$$

which shows that we have an effective attenuation of the form of Eq. (1) with $\alpha = -1$ and no effective dispersion.

These two cases (mixing and regular) are the ones observed with standard models of random media and they have been extensively studied [4, 16]. As we will see in the next subsections, the picture becomes more interesting when non-mixing or rough random media are considered.

3.4. *Random Media with Long-range Correlation Properties*

This is the regime in which the random medium has the H'-long-range correlation property, $H' \in (1/2, 1)$. We first consider the binary medium model described in (17-19). We find using Eq. (19) and [21, formula 3.761] that

$$\begin{aligned}\sigma^{-2}Q_{e,l}^{-1}(v) = {} & \frac{v^{2-2H'}}{2^{2H'}(3-2H')}\Gamma(2H'-1)\cos((H'-1/2)\pi) \\ & + \frac{v}{2(3-2H')}\left(\frac{\sin(2v)}{2v} + (1-H')\frac{\sin^2(v)}{v^2}\right) \\ & - \frac{v}{2(3-2H')}\int_0^1 z^{2H'-2}\cos(2vz)dz\,,\end{aligned} \tag{44}$$

or equivalently:

$$\sigma^{-2}Q_{\rm e,l}^{-1}(v) = \frac{1-H'}{4(3-2H')}\frac{1}{v} - \frac{1-H'}{4}\frac{1}{v}\int_1^\infty z^{2H'-4}\cos(2vz)dz\,. \qquad (45)$$

The first form is useful to get an expansion for small v, the second form is useful to get an expansion for large v.

The effective damping function is shown in Figure 5 for several H' values, top plot. In the figure $H' = .55, .75$, and $.95$ correspond respectively to the dashed blue, solid black, and dash-dotted red lines.

The dispersion function can be expressed as

$$\begin{aligned}\sigma^{-2}\mathcal{D}_{\rm e,l}(v) = {} & \frac{v^{2-2H'}}{2^{2H'}(3-2H')}\Gamma(2H'-1)\sin((H'-1/2)\pi) \\ & + \frac{v}{2}\left(\frac{2-2H'}{3-2H'}\left(\frac{\cos(2v)}{2v} - \frac{\sin(2v)}{(2v)^2}\right) + \frac{\sin^2(v)}{v}\right) \\ & - \frac{v}{2(3-2H')}\int_0^1 z^{2H'-2}\sin(2vz)dz\,, \end{aligned} \qquad (46)$$

or equivalently

$$\sigma^{-2}\mathcal{D}_{\rm e,l}(v) = \frac{1}{4} - \frac{1-H'}{4v}\int_1^\infty z^{2H'-4}\sin(2vz)dz\,. \qquad (47)$$

The effective dispersion function is shown in Figure 6 for several H' values, top plot. In the figure $H' = .55, .75$, and $.95$ correspond respectively to the dashed blue, solid black, and dash-dotted red lines.

We remark that when we only consider low frequencies that probe mainly the tail of the covariance function of the medium we find:

$$\begin{aligned}\sigma^{-2}Q_{\rm e,l}^{-1}(v) &\simeq v^{2-2H'}\frac{\Gamma(2H'-1)\cos((H'-1/2)\pi)}{2^{2H'}(3-2H')}\,, \qquad v \ll 1\,, \\ \sigma^{-2}\mathcal{D}_{\rm e,l}(v) &\simeq v^{2-2H'}\frac{\Gamma(2H'-1)\sin((H'-1/2)\pi)}{2^{2H'}(3-2H')}\,, \qquad v \ll 1\,. \end{aligned}$$

Thus, in this regime the damping exponent α in Eq. (1) is $2-2H' \in (0,1)$. We compute the damping and dispersion exponents:

$$\alpha(v) = \frac{v\partial_v\left[Q_{\rm e}^{-1}(v)\right]}{Q_{\rm e}^{-1}(v)}\,, \quad \beta(v) = \frac{v\partial_v\left[\mathcal{D}_e(v)\right]}{\mathcal{D}_e(v)}\,, \qquad (48)$$

via a numerical approximation and plot them in Figure 5 and 6 bottom plots. Note that in the high-frequency regime the wave probes the affine (regular) decay of the covariance function at the origin corresponding to a damping exponent of -1. This can be seen from the alternative representations (45) and (47):

$$\begin{aligned}\sigma^{-2}Q_{\rm e,l}^{-1}(v) &\simeq \frac{1-H'}{4(3-2H')}\frac{1}{v}\,, \qquad v \gg 1\,, \\ \sigma^{-2}\mathcal{D}_{\rm e,l}(v) &\simeq \frac{1}{4}\,, \qquad v \gg 1\,. \end{aligned}$$

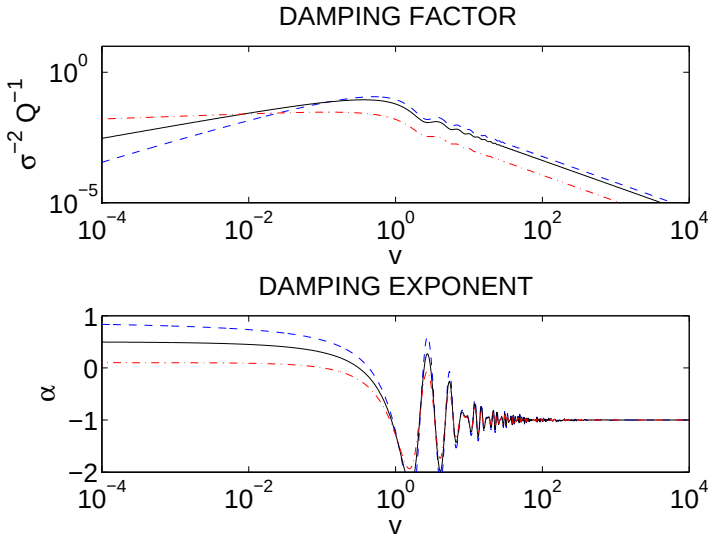

Figure 5. The normalized damping factor $\sigma^{-2}Q_{\mathrm{e,l}}^{-1}(v)$, top plot, and the damping exponent $\alpha(v)$, bottom plot. Here $H' = .55, .75$, and $.95$ correspond respectively to the dashed blue, solid black, and dash-dotted red lines.

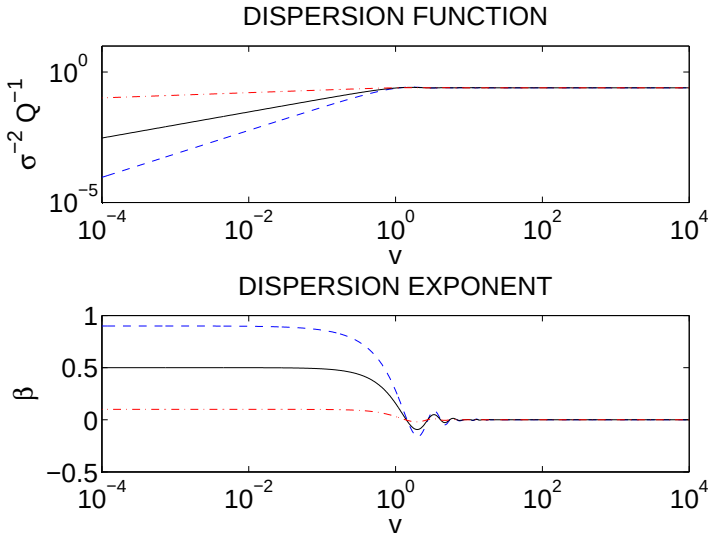

Figure 6. The normalized dispersion function $\sigma^{-2}\mathcal{D}_{\mathrm{e,l}}(v)$, top plot, and the dispersion exponent $\beta(v)$, bottom plot. Here $H' = .55, .75$, and $.95$ correspond respectively to the dashed blue, solid black, and dash-dotted red lines.

We finally remark on the general long range model in Eq. (10). We have for $1/2 < H' < 1$ (using [21, formula 3.761]):

$$Q_{\mathrm{e,l}}^{-1}(v) \simeq v^{2-2H'} \frac{r_{H'}\Gamma(2H'-1)\cos((H'-1/2)\pi)}{2^{2H'-2}}, \qquad v \ll 1$$

$$\mathcal{D}_{\mathrm{e,l}}(v) \simeq v^{2-2H'} \frac{r_{H'}\Gamma(2H'-1)\sin((H'-1/2)\pi)}{2^{2H'-2}}, \qquad v \ll 1\,.$$

The binary medium model described in (17-19) is just one particular model with long-range correlation properties for which the following behavior can be observed. Wave propagation in a random medium with long-range correlations exhibits

frequency-dependent attenuation that is characterized by a power law of the form of Eq. (1) with the exponent $\alpha = 2 - 2H'$ ranging from 0 to 1 in the low-frequency regime. Moreover, the propagation is associated with a dispersive effect.

3.5. *Random Media with Short-range Correlation Properties*

This is the regime in which the random medium possesses the H-short-range correlation property, $H \in (0, 1/2)$. We first consider the binary medium model described in (20-24). We denote $\delta = \ell_{\rm i}/\ell_{\rm c}$. From Eq. (24) we find

$$\sigma^{-2} Q^{-1}_{\rm e,s}(v) = \frac{v}{2(1-2H)(1-\delta^{2H})}\Big\{ -\int_\delta^1 z^{2H}\cos(2vz)dz + \frac{\sin(2v)}{2v} - H\frac{\sin^2 v}{v^2} \\ -\delta^{2H+1}\frac{\sin(2v\delta)}{2v\delta} + H\delta^{2H+1}\frac{\sin^2(v\delta)}{(v\delta)^2}\Big\}, \quad (49)$$

or equivalently:

$$\sigma^{-2} Q^{-1}_{\rm e,s}(v) = \frac{H}{4(1-\delta^{2H})v}\Big\{ -\int_\delta^1 z^{2H-2}\cos(2vz)dz + \frac{\delta^{2H-1}-1}{1-2H}\Big\}. \quad (50)$$

The first form is useful to get an expansion for small v, while the second form is useful to get an expansion for large v.

For this model we can now differentiate three regimes: (i) $v \ll 1$: the low-frequency regime, (ii) $1 \ll v \ll 1/\delta$: the mid-frequency regime, (iii) the high-frequency regime $v \gg 1/\delta$.

Consider first the low-frequency regime, we have

$$\sigma^{-2} Q^{-1}_{\rm e,s}(v) \simeq v\frac{H(1-\delta^{1+2H})}{2(1+2H)(1-\delta^{2H})}, \qquad v \ll 1.$$

Consider next the mid-frequency range, then we can write

$$\sigma^{-2} Q^{-1}_{\rm e,s}(v) \simeq v^{-2H}\frac{\Gamma(1+2H)\sin(H\pi)}{2^{2+2H}(1-2H)(1-\delta^{2H})}, \qquad 1 \ll v \ll 1/\delta. \quad (51)$$

Consider finally the high-frequency regime, in this case:

$$\sigma^{-2} Q^{-1}_{\rm e,s}(v) \simeq v^{-1}\frac{H(\delta^{2H-1}-1)}{4(1-2H)(1-\delta^{2H})}, \qquad v \gg 1/\delta.$$

The effective damping function is shown in Figure 7 for several H values, top plot. In the figure $H = .05, .25$, and $.45$ correspond respectively to the dashed blue, solid black, and dash-dotted red lines and in all cases $\delta = 10^{-4}$. The bottom plot shows the corresponding damping exponents $\alpha(v)$. In the figure we can clearly identify the three regimes.

The effective dispersion function is given by

$$\sigma^{-2}\mathcal{D}_{\rm e,s}(v) = \frac{1}{4(1-2H)(1-\delta^{2H})}\Big\{ -2v\int_\delta^1 z^{2H}\sin(2vz)dz + 2H\big(\frac{\sin(2v)}{2v} - 1\big) \\ -\big(\cos(2v)-1\big) - 2H\delta^{2H}\big(\frac{\sin(2v\delta)}{2v\delta} - 1\big) + \delta^{2H}\big(\cos(2v\delta)-1\big)\Big\}, \quad (52)$$

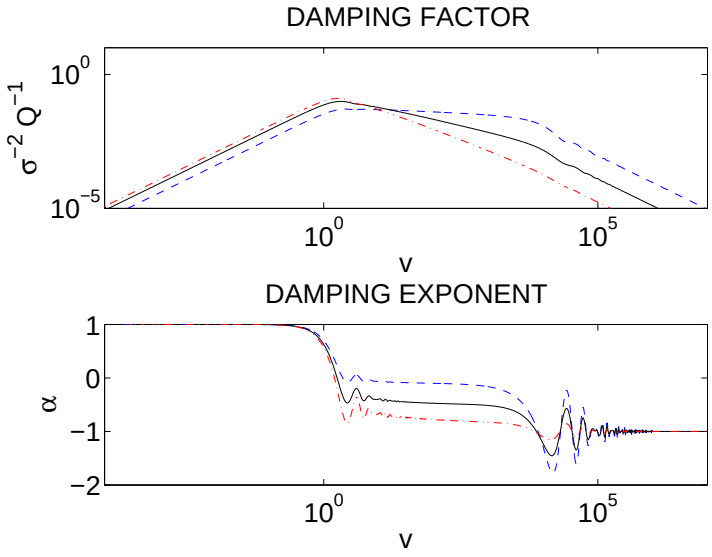

Figure 7. The normalized damping factor $\sigma^{-2}Q_{\rm e,s}^{-1}(v)$, top plot, and the damping exponent $\alpha(v)$, bottom plot. Here $H = .05, .25$, and $.45$ correspond respectively to the dashed blue, solid black, and dash-dotted red lines, and in all cases $\delta = 10^{-4}$.

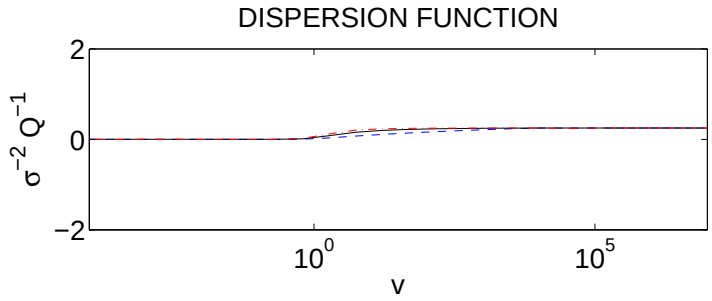

Figure 8. The normalized dispersion function $\sigma^{-2}\mathcal{D}_{\rm e,s}(v)$. Here $H = .05, .25$, and $.45$ correspond respectively to the dashed blue, solid black, and dash-dotted red lines, and in all cases $\delta = 10^{-4}$.

or equivalently by

$$\sigma^{-2}\mathcal{D}_{\rm e,s}(v) = \frac{1}{4} - \frac{H}{4(1-\delta^{2H})v}\int_\delta^1 z^{2H-2}\sin(2vz)dz\,. \tag{53}$$

In the low-frequency regime, we have

$$\sigma^{-2}\mathcal{D}_{\rm e,s}(v) \simeq v^2\frac{H(1-\delta^{2+2H})}{6(1+H)(1-\delta^{2H})}\,, \qquad v \ll 1\,.$$

In the mid- and high-frequency ranges, we have

$$\sigma^{-2}\mathcal{D}_{\rm e,s}(v) \simeq \frac{1}{4}\,, \qquad v \gg 1\,.$$

The effective dispersion function is plotted in Figure 8 for several H values. In the figure $H = .05, .25$, and $.45$ correspond respectively to the dashed blue, solid black, and dash-dotted red lines, and in all cases $\delta = 10^{-4}$.

The binary medium model described in (20-24) is only one particular model amongst the media who possess the short-range correlation property. It is shown in Appendix B [19] that the power law scaling for the attenuation is valid for general covariance functions of the form in Eq. (11) with $0 < H < 1/2$ satisfying certain regularity properties in the high-frequency regime $v = |\omega|\ell_c/c_0 \gg 1$: As shown in Appendix B [19] we have for the general model Eq. (11)

$$\sigma^{-2} Q_e^{-1}(v) \simeq v^{-2H} \frac{d_H \Gamma(1+2H)\sin(\pi H)}{2^{2H}}, \qquad v \gg 1, \tag{54}$$

$$\sigma^{-2} \mathcal{D}_e(v) \simeq v^{-2H} \frac{d_H \Gamma(1+2H)\cos(\pi H)}{2^{2H}}, \qquad v \gg 1, \tag{55}$$

corresponding to Eq. (51) with here $\sigma^2 = \phi(0)$. The above shows that wave propagation in random media with short-range correlation properties exhibits frequency-dependent attenuation that is characterized by a power law of the form of Eq. (1) with the exponent $\alpha = -2H$ ranging from -1 to 0 in the high-frequency range.

3.6. *Random Media with Short-Range and Long-Range Properties*

Let us consider a medium with both short-range and long-range correlation properties, such as the binary medium addressed in Subsection 2.3. In this case we can distinguish three frequency bands for which the exponent of the power-law frequency-dependent attenuation takes values $\alpha \in (0,1)$ for the low-frequency band (or large wavelengths beyond the outer scale ℓ_c), $\alpha \in (-1,0)$ for the mid-frequency band (or wavelengths within the inertial range between ℓ_i and ℓ_c), and $\alpha = -1$ for the high-frequency band (or wavelengths below the inner scale ℓ_i):
- For relatively low frequencies such that $v \ll 1$, the H'-long-range correlation property gives an exponent $\alpha = 2 - 2H' \in (0,1)$.
- For relatively high frequencies such that $1 \ll v \ll 1/\delta$, the H-short-range correlation property gives an exponent $\alpha = -2H \in (-1,0)$.
- For very high frequencies such that $v \gg 1/\delta$, the regular property gives an exponent $\alpha = -1$.

Consider the particular case of the binary medium described in (26-32). We can write the resulting damping function as:

$$\sigma^{-2} Q_{e,ls}^{-1}(v) = \sigma^{-2} \left\{ (1+\mathcal{C})^{-1} Q_{e,l}^{-1}(v) + (1+\mathcal{C}^{-1})^{-1} Q_{e,s}^{-1}(v) \right\},$$

for

$$\mathcal{C} = \mathcal{C}(a,\delta,H,H') = \frac{(1-2H)(2-2H')(1-a\delta^{1-2H})(1-\delta^{2H})}{a2H(3-2H')(1-\delta^{1-2H})},$$

which is an order one mixing factor. For instance, if a is given by (27) and $\delta \ll 1$, then $\mathcal{C} = (1-H')/H$. Note that $Q_{e,l}^{-1}(1)/Q_{e,s}^{-1}(1)$ is an order one factor and we have indeed that the damping exponent is: $\alpha = 2 - 2H'$ for $v \ll 1$; $\alpha = -2H$ for

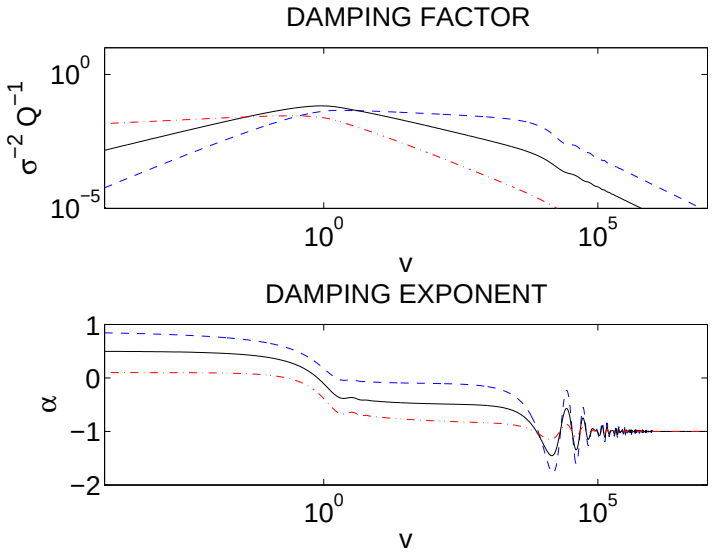

Figure 9. The normalized damping factor $\sigma^{-2}Q^{-1}_{\rm e,ls}(v)$, top plot, and the damping exponent $\alpha(v)$, bottom plot. Here (H, H') are $(.05, .55)$, $(.25, .75)$, and $(.45, .95)$ for respectively the dashed blue, solid black, and dash-dotted red lines, and in all cases $\delta = 10^{-4}$.

$1 \ll v \ll 1/\delta$, and $\alpha = -1$ for $v \gg 1/\delta$. More exactly, if $\delta \ll 1$, we have:

$$\sigma^{-2}Q^{-1}_{\rm e,ls}(v) \approx \begin{cases} v^{2-2H'} \dfrac{\Gamma(2H'-1)\cos((H'-1/2)\pi)}{2^{2H'}(3-2H')(1+\mathcal{C})} & , \quad v \ll 1 \ , \\ v^{-2H} \dfrac{\Gamma(1+2H)\sin(H\pi)}{2^{2+2H}(1-2H)(1+\mathcal{C}^{-1})} & , \quad 1 \ll v \ll 1/\delta \ , \\ v^{-1} \dfrac{H\delta^{2H-1}}{4(1-2H)(1+\mathcal{C}^{-1})} & , \quad v \gg 1/\delta \ . \end{cases} \tag{56}$$

We show $Q^{-1}_{\rm e,ls}$ in Figure 9 for (H, H') being $(.05, .55)$, $(.25, .75)$, and $(.45, .95)$ by the dashed blue, solid black, and dash-dotted red lines respectively, moreover $\delta = 10^{-4}$. In the figure we can clearly identify the three frequency regimes separated by "transition zones".

3.7. *Observed Damping Exponents*

Summarizing the above we see that our modeling naturally leads to three regimes of propagation: high-, mid- and low- frequency ranges with associated damping factors and characteristic frequency exponent scaling for these. We stress that here we have considered apparent attenuation only. In real media, to what extent observed attenuation is intrinsic or apparent is in many cases still an open question.

In [34] the authors discuss propagation in the mantle and motivate there the use of a one-dimensional model for the microstructure. As mentioned, they quote an exponent about $\alpha \approx .4$ for very low frequencies below .001 Hz, corresponding to long range dependence and $H' = .8$. Moreover, a mid frequency range of .001-1 Hz with α ranging from -.4 to 0 depending on the type of wave mode, corresponding to $0 < H < .2$. Finally, somewhere above 1 Hz they report a corner past which the exponent is close to -1. This picture is consistent with the quantitative results seen in Figure 9.

In [31] some typical values for the damping exponent for sound propagation in sea

water and air are quoted, corresponding to $\alpha \approx 1$ for low frequencies, $\alpha \approx -.5$ for medium frequencies, and $\alpha \approx -1$ for high frequencies, which in turn is consistent with the picture in Figure 7 and $H = .25$, see [1, 5].

An important motivation for studying frequency-dependent attenuation is to understand attenuation in human tissue. In [6] such attenuation is discussed in the context of photoacoustic tomography, moreover, it is discussed how one can correct for it to enhance medical imaging technology. The authors report a damping exponent in the range .31 to .36 in fat tissue just under the skin. Moreover, in [24] a damping exponent close to 0 was measured in the context of different types of organ tissue and it was hypothesized that the differentiation of damping exponent with tissue type could be used for classification.

Finally let us mention that the multiscale and turbulent atmosphere corresponds to $H = 1/3$ (Kolmogorov's scaling law) in the internal range, the scale range delineated by the inner out outer scales. In this case the low-frequency regime is referred to as the scales beyond the "outer scale", the mid-frequency regime as the "inertial range" and the high-frequency regime as the scales below the "inner scale". Atmospheric turbulence data was analyzed in [33] giving an estimate of $H \approx 1/3$ in an inertial range, an inertial range that actually may vary somewhat with location.

We stress that the theoretical results quoted above were derived in a layered or one-dimensional medium, however, some aspects of this theory carry over to 3D wave propagation [18] and more details on this will be reported elsewhere.

3.8. *Comparison with anelastic attenuation*

We have discussed how observed wave attenuation can be explained via a scattering model. Clearly wave attenuation can also be caused by anelastic attenuation. To complement the above discussion we therefore briefly comment on modeling of anelastic attenuation. A variety of anelastic physical processes can contribute to attenuation in a solid: motions of point defects, dislocations, grain boundaries, and so on [2, Chapter 14]. The standard linear solid model or viscoelastic model gives a Q factor of the Debye form:

$$Q^{-1}(\omega) = 2Q_{\max}^{-1} \frac{\omega\tau}{1+\omega^2\tau^2},$$

where τ is the relaxation time of the mechanism under consideration and $Q_{\max}^{-1}$ is the maximal value of Q^{-1} reached at $\omega = \tau^{-1}$. However, as mentioned in the introduction anf first obserevd in [26], it appears that the Q-factor is only weakly frequency-dependent over most of the seismic band. A weak frequency dependence can only be explained by invoking a distribution of relaxation times. A distribution of dislocation lengths, grain sizes and so on may be involved [23, 29]. Such a superposition of relaxation mechanisms gives a Q factor of the form

$$Q^{-1}(\omega) = 2Q_{\max}^{-1} \int D(\tau) \frac{\omega\tau}{1+\omega^2\tau^2} d\tau,$$

where $D(\tau)$ is called the retardation spectrum. The form of the retardation spectrum in the absorption-band model (ABM) is [3]

$$D(\tau) = \frac{\alpha}{\tau_2^\alpha - \tau_1^\alpha} \tau^{\alpha-1} \mathbf{1}_{[\tau_1,\tau_2]}(\tau),$$

for $\alpha \in (0,1)$ and for $\tau_1 < \tau_2$ the shortest and longest relaxation times of the mechanism under consideration. When $\tau_1 \ll \tau_2$, we have three regimes: $Q^{-1}(\omega) \sim \omega$ for $\omega\tau_1 \ll 1$, $Q^{-1}(\omega) \sim \omega^\alpha$ for $\omega\tau_1 \ll 1 \ll \omega\tau_2$, and $Q^{-1}(\omega) \sim \omega^{-1}$ for $\omega\tau_2 \gg 1$. This result holds for all relaxation mechanisms [2, Chapter 14].

Remember that, at frequencies larger than about 1Hz, Q^{-1} appears to decrease linearly with frequency [10, 12]. This is consistent with the behavior expected from the ABM model on the high-frequency side of a relaxation band. At frequencies smaller than $< 10^{-3}$Hz it is reported for body waves that $Q^{-1}(\omega) \sim \omega^\alpha$ with $\alpha \simeq 0.4$ [27], while at intermediate frequencies one observes $Q^{-1}(\omega) \sim \omega^\alpha$ with $\alpha \in (-0.4, 0)$ in the range $(10^{-3}, 1)$Hz [10, 36]. These two regimes are not really consistent with the ABM model which predicts an exponent $\alpha = 1$ for very low frequencies and $\alpha \in (0,1)$ at intermediate frequencies: One would need to extend the ABM model to negative α's to produce the observed decay at intermediate frequencies and to imagine multi-band distributions of relaxation times that would produce an anomalous behavior of the Q factor at low frequencies.

To summarize, anelastic attenuation can explain a frequency dependence of the Q factor. In particular the ABM model is a phenomenological model that can reproduce the observed frequency dependence of the Q factor provided the retardation spectrum has a special form. On the other hand, scattering induced attenuation can be introduced from first principles, that is to say, it follows directly from the wave equation, it requires heterogeneities compatible with the observed attenuation [34], and it produces a frequency dependent Q factor that naturally follows the observed behaviors as explained in our paper. It also explains in a simple and natural way why bulk attenuation seems negligible as discussed in [34]. Scattering induced attenuation is therefore a natural candidate to explain at least partially the apparent seismic attenuation.

Note that the dispersion produced by an ABM model and by a scattering induced phenomenon would be of the same form as soon as they produce the same frequency dependence of the Q factor, because both mechanisms are causal and therefore respect Kramers-Kronig relations.

4. Conclusion

In this paper we have shown that wave propagation is a randomly scattering medium can lead to effective properties that exhibit power-law frequency dependence of the attenuation coefficient with an exponent in the range $(-1, 1)$.

(i) In a random medium with a covariance function that decays for $|z|$ larger than ℓ_c as $|z|^{2H'-2}$, $H' \in (1/2, 1)$, the attenuation has a power law frequency-dependence of the form $Q^{-1}(\omega) \approx \omega^\alpha$ with $\alpha = 2 - 2H' \in (0,1)$ for low frequencies (smaller than c_0/ℓ_c).

(ii) In a random medium with a covariance function that behaves like $1 - d_H|z|^{2H}$, $H \in (0, 1/2)$, in an interval $|z| \in (\ell_i, \ell_c)$, then the attenuation has a power law frequency-dependence of the form $Q^{-1}(\omega) \approx \omega^\alpha$ with $\alpha = -2H \in (-1, 0)$ for mid frequencies (in the range $(c_0/\ell_c, c_0/\ell_i)$).

(iii) In a random medium with a covariance function that decays like $1 - d_{1/2}|z|$ for $|z|$ smaller than ℓ_i, then the attenuation has a power law frequency-dependence of the form $Q^{-1}(\omega) \approx \omega^\alpha$ with $\alpha = -1$ for high frequencies (larger than c_0/ℓ_i).

A random medium can possess the multiscale behavior (i-ii-iii) as for instance the simple binary medium described in Subsection 2.3, which gives different exponents for different frequency bands, and one can naturally get the same power dependences of the frequency-dependent attenuation as in the experimental observations.

The fact that simple medium models reproduce accurately the complex frequency behavior of the apparent attenuation observed for seismic waves propagating in the mantle can be interpreted in favor of the hypothesis that the observed seismic attenuation comes from multiple scattering [34].

In all cases a special frequency-dependent phase is associated to the frequency-dependent attenuation and it ensures that causality and Kramers-Kronig relations are respected. Effective fractional wave equations can be written that have the form of equations studied in the literature in the context of wave propagation in lossy media [9, 19, 22, 39].

Acknowledgements

This work was partly supported by AFOSR grant # FA9550-11-1-0176 and by ERC Advanced Grant Project MULTIMOD-267184. We thank Jean-Paul Montagner for useful and stimulating discussions.

References

[1] M. Ainslie and J. G. McColm, "A simplified formula for viscous and chemical absorption in sea water", J. Acoust. Soc. Am. **103** 1671–172 (1998).
[2] D. L. Anderson, "Theory of the Earth," Blackwell Scientific Publications, Boston, 1989.
[3] D. L. Anderson and J. W. Given, "Absorption band Q model for the Earth," J. Geophys. Res. **87**, 3893–3904 (1982).
[4] M. Asch, W. Kohler, G. Papanicolaou, M. Postel, and B. White, "Frequency content of randomly scattered signals," SIAM Review **33**, 519–626 (1991).
[5] H. Bass, L. sutherland, A. Zuckerwar, D. Blackstock, and D. Hester, "Atmospheric absorption of sound: Further developments", J. Acous. Soc. Am. **97**, 680–683 (1995).
[6] P. Burgholzer, H. Roitner, J. Bauer-Marschallinger, and G. Paltauf, "Image reconstruction in photoacoustic tomography using integrating detectors accounting for frequency-dependent attenuation," Proc. SPIE 7564, Photons Plus Ultrasound: Imaging and Sensing (2010).
[7] R. Burridge and H. W. Chang, "Multimode one-dimensional wave propagation in a highly discontinuous medium," Wave Motion **11**, 231–249 (1989).
[8] R. Burridge, G. Papanicolaou, and B. White, "One-dimensional wave propagation in a highly discontinuous medium," Wave Motion **10**, 19–44 (1988).
[9] W. Chen and S. Holm, "Modified Szabo's wave equation models for lossy media obeying frequency power law," J. Acoust. Soc. Am. **114**, 2570–2574 (2003).
[10] G. L. Choy and V. F. Cormier, "Direct measurement of the mantle attenuation operator from broadband P and S waveforms," J. Geophys. Res. **91**, 7326–7342 (1986).
[11] J.-F. Clouet and J.-P. Fouque, "Spreading of a pulse traveling in random media," Ann. Appl. Probab. **4**, 1083–1097 (1994).
[12] V. F. Cormier, "Seismic viscoelastic attenuation," in Encyclopedia of Solid Earth Geophysics, H. K. Gupta (ed.), Springer, Dordrecht, 2011, pp. 1279–1290.
[13] S. Dolan, C. Bean, and B. Riollet, "The broad-band fractal nature of heterogeneity in the upper crust from petrophysical logs," Geophys. J. Int. **132**, 489–507 (1998).
[14] A. Fannjiang and K. Sølna, "Scaling limits for wave beams in atmospheric turbulence," Stoch. Dyn. **4**, 135–151 (2004).
[15] W. Feller, *An introduction to probability theory and its applications*, Vol. 2, Chap. 11 (Wiley, New York, 1971).
[16] J.-P. Fouque, J. Garnier, G. Papanicolaou, and K. Sølna, *Wave propagation and time reversal in randomly layered media* (Springer, New York, 2007).

[17] A. E. Gargett, "The scaling of turbulence in the presence of stable stratification," J. Geophys. Res. **93**, 5021–5036 (1988).
[18] J. Garnier and K. Sølna, "Coupled wideangle wave approximations," SIAM Multiscale Model. Simul. **10**, 217–244 (2012).
[19] J. Garnier and K. Sølna, "Effective fractional acoustic wave equations in random multiscale media", J. Acoust. Soc. Am. **127**, 62–72 (2010).
[20] J. Garnier and K. Sølna, "Pulse propagation in random media with long-range correlation," SIAM Multiscale Model. Simul. **7**, 1302–1324 (2009).
[21] I. S. Gradshteyn and I. M. Ryzhik, *Table of integrals, series, and products* (Academic Press, San Diego, 1980).
[22] A. Hanyga and V. E. Rok, "Wave propagation in micro-heterogeneous porous media: A model based on an integro-differential wave equation," J. Acoust. Soc. Am. **107**, 2965–2972 (2000).
[23] D. D. Jackson and D. L. Anderson, "Physical mechanisms of seismic-wave attenuation," Rev Geophys. Space Phys. **8**, 1–63 (1970).
[24] M. P. Kadaba, P. K. Bhagat, and V. C. Wu, "Attenuation and backscattering of ultrasound in freshly excised animal tissues," IEEE Trans Biomed Eng. **27**, 76–83 (1980).
[25] L. Klimes, "Correlation functions of random media," Pure and Applied Geophysics **159**, 1811–1831 (2002).
[26] L. Knopoff, "Q," Rev. Geophys. **2**, 625–660 (1964).
[27] V. Lekic, J. Matas, M. Panning, and B. Romanowicz, "Measurements and implications of frequency dependence of attenuation," Earth and Planet. Sci. Lett. **282**, 285–293 (2009).
[28] P. Lewicki, R. Burridge, and M. De Hoop, "Beyond effective medium theory: pulse stabilization for multimode wave propagation in high-contrast layered media," SIAM J. Appl. Math. **56**, 256–276 (1996).
[29] H. P. Liu, D. L. Anderson, and H. Kanamori, "Velocity dispersion due to anelasticity: implication for seismology and mantle composition," Geophys. J. Roy. Astron. Soc. **47**, 41–58 (1976).
[30] A. Nachbin and K. Sølna, "Apparent diffusion due to topographic microstructure in shallow waters," Phys. Fluids **15**, 66–77 (2003).
[31] S.P. Näsholm and S. Holm, "On fractional Zener elastic wave equation," Calc. Appl. Anal. **16**, 26–50 (2013).
[32] R. F. O'Doherty and N. A. Anstey, "Reflections on amplitudes," Geophysical Prospecting **19**, 430–458 (1971).
[33] G. Papanicolaou and K. Sølna, "Wavelet based estimation of Kolmogorov turbulence", In: Long-range Dependence: Theory and Applications. Editors P. Doukhan, G. Oppenmeim and M. S. Taqqu, (2002).
[34] Y. Ricard, S. Durand, J.-P. Montagner, and F. Chambat, "Is there seismic attenuation in the mantle?", Earth Planet. Sci. Lett. **388**, 257–264 (2014).
[35] M. Sahimi and S. E. Tajer, "Self-affine fractal distributions of the bulk density, elastic moduli, and seismic wave velocities of rock," Phys. Rev. E **71**, 046301 (2005).
[36] A. Shito, S. I. Karato, and J. Park, "Frequency dependence of Q in Earth's upper mantle inferred from continuous spectra of body waves," Geophys. Res. Lett. **31**, L12603 (2004).
[37] C. Sidi and F. Dalaudier, "Turbulence in the stratified atmosphere: Recent theoretical developments and experimental results," Adv. in Space Res. **10**, 25–36 (1990).
[38] K. Sølna and G. C. Papanicolaou, "Ray theory for a locally layered medium," Waves in Random Media **10**, 151–198 (2000).
[39] T. L. Szabo, "Time domain wave equations for lossy media obeying a frequency power law," J. Acoust. Soc. Am. **96**, 491–500 (1994).